Published in: European Journal of Inorganic Chemistry; Article first published online: 23 DEC 2015;
DOI: 10.1002/eiic.201501168

Hierarchical meso-meso and macro-mesoporous silica templated by mixtures of polyoxyethylene fluoroalkyl ether and triblock copolymer

A. May-Masnou[a,b], M.J. Stébé[a] and J.L. Blin[a*]

[a]: Université de Lorraine/CNRS, SRSMC, UMR7565, F-54506 Vandoeuvre-lès-Nancy cedex, France
[b]: Chemical Engineering Department, Chemistry Faculty, Universitat de Barcelona, Martí i Franquès 1-11, 08028, Barcelona, Catalonia, Spain

* Corresponding authors:

Pr. Jean-Luc Blin
Université de Lorraine
SRSMC UMR 7565
Faculté des Sciences et Technologies
BP 70239
F-54506 Vandoeuvre-lès-Nancy cedex, France
Tel. +33 3 83 68 43 70
E-mail: Jean-Luc.Blin@univ-lorraine.fr

http://www.srsmc.univ-lorraine.fr

Keywords: Hierarchical porosity, Mixed micellar solutions, Fluorinated surfactant, Pluronic, Emulsions

Abstract

We report here the synthesis of different kinds of hierarchical porous silica materials by using mixtures of an amphiphilic block copolymer (Pluronic P123) and a nonionic fluorinated surfactant. In particular, we have taken advantage of the difference in polarities between the two compounds to design dual-mesoporous materials through the cooperative templating mechanism (CTM). We have undertaken a complete study of this system by varying the composition of the mixed micelles and the synthesis conditions. We have shown that both the dual-mesoporosity and the mesopore ordering are favored when materials are prepared with fluorinated-rich and P123-rich micelles. However, when the rich-Pluronic micelles predominate the mesostructure is less organized and the dual-porosity depends on the P123 content.

Then by incorporating perflurodecalin (PFD) in the surfactant mixture concentrated emulsions are formed and hierarchical macro-mesoporous materials have been prepared by combining the CTM and the emulsion templating mechanism.

Introduction

Porous materials have found wide applications in many traditional fields such as catalysis, adsorption, electronics and environmental technology because of their high surface area coupled with many other physical and chemical properties[1-5]. Among the various methods for creating pores, the surfactant templating strategy affords a variety of porous networks with a wide range of pore sizes, well-defined morphologies on controllable length scales and various chemical functionalities to match the needs of different applications. As a matter of fact, in water, eventually in the presence of oil, surfactant molecules can pack together to form various organized molecular systems (OMS). Associated with the sol-gel process, these OMS lead to the formation of various porous materials such as the silica ones. Depending on the building blocks, i.e. micelles, microemulsions, liquid crystals or emulsions, different kinds of porous materials can be designed. Micelles and liquid crystals lead to ordered mesoporous materials through the cooperative (CTM)[6-10] and the transcriptif (LCT) mechanisms[11-15], respectively. For example, El-Safty et *al.* have reported the synthesis in strong acid conditions of nanometer-sized silica monolith by using lyotropic liquid crystals mesophases of polyoxyethylene alkyl ether, Triton, Tween and triblock copolymers type surfactants as a structure-directing agent[12,13]. The oil solubilization into the surfactant systems can give swollen micelles or microemulsions, which in the presence of the silica precursor give rise to large pore ordered mesoporous materials[16-21]. The mesopore expansion can occur either through a swelling of the micelles or of the hybrid mesophase. Further addition of oil involves the formation of emulsions, and using them as template, macroporous materials can be prepared[22-24].

In addition to these mono-modal materials, the development of hierarchically ordered structures at multiple length scales is also of particular interest for catalysis and for the engineering of pore systems[25,26]. Indeed, it was reported that a hierarchical combination of

mesopores reduces transport limitations in catalysis, resulting in higher activities and better controlled selectivity[27]. Therefore, over the past few years the development of these hierarchically ordered structures at multiple length scales has attracted much attention and materials with a micro-macroporous or a meso-macroporous structure have been synthesized using multiple templates through either soft or hard templating methods[28-34].

However, emulsions templating is perhaps most general and has been used to produce macroporous silica, titania and zirconia[35]. Comparing with the micro-mesoporous or the meso-macroporous materials, the systems having two types of mesopores are barely investigated. On the condition that the two templates have hydrophobic chains with different sizes, mixtures of hydrogenated and fluorinated surfactants are excellent candidates to design these dual-mesoporous silica materials via a one-step synthesis process. In a previous letter [36], taking advantage of the behavior of mixed hydrogenated/fluorinated systems, we have demonstrated that dual-mesoporous materials can be obtained from a mixture of the polyoxyethylene fluoroalkyl ether $R^F_8(EO)_9$ and the Pluronic (P123). It should be noted that syntheses have been performed only under the experimental conditions that give well ordered mesostructures using the pure fluorinated surfactant. Here, to better address the formation of these dual-mesoporous materials, we have investigated in detail these systems. In particular we have varied the composition of the micelles and the total concentration of surfactant. This has led us to consider both fluorinated-rich and Pluronic-rich systems. In addition we have also incorporated a fluorinated oil to prepare emulsions, which have been used to template macro-mesoporous materials.

Results and discussion

Micellar solution in the $R^F_8(EO)_9$-P123 mixed system:

When mesoporous materials are prepared through the CTM mechanism, the surfactant has to form micelles in water. To know if this criterion is respected by the $R^F_8(EO)_9$-P123 mixed system, first we looked at the $R^F_8(EO)_9$/P123/water ternary phase diagram (Fig. 1).

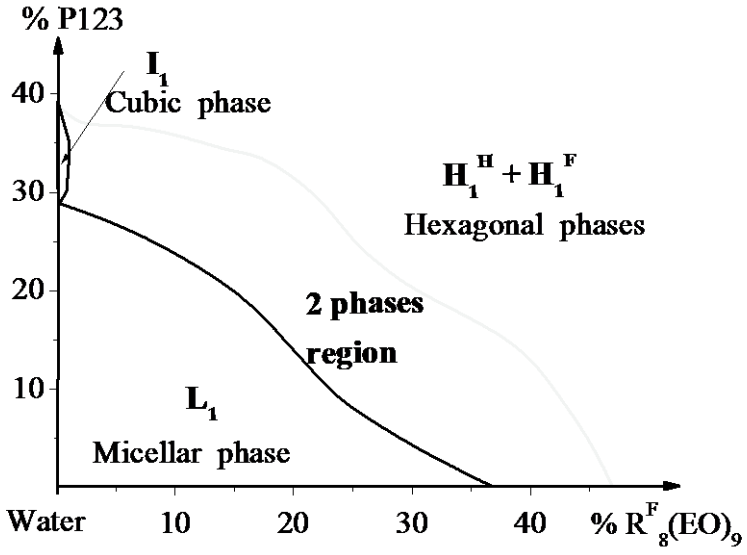

Figure 1: Partial composition (wt.%) phase diagram of the $R^F_8(EO)_9$/P123/water system at 20°C.

In the water rich part of the diagram and at least up to a global surfactant [P123 + $R^F_8(EO)_9$] concentration of 30 wt.%, a direct micellar phase (L_1) is detected whatever the proportion between $R^F_8(EO)_9$ and P123. A liquid crystal domain, for which the hexagonal-type structure (H_1) is the predominant phase, appears beyond 50 wt.% of total surfactant. This hexagonal region is mainly composed of a biphasic mixture of one fluorocarbon-rich H_1^F hexagonal phase in equilibrium with one hydrocarbon-rich H_1^H hexagonal phase. Each phase can incorporate only a weak fraction of the second surfactant. However, since our goal is to synthesize the dual-mesoporous materials through the CTM mechanism, we have not gone deeper on the characterization of H_1 and we have focused our investigations on the micellar region. For a surfactant concentration located at around 1 wt.%, the hydrodynamic diameters,

measured by DLS, of both the pure fluorinated and Pluronic micelles are equal to 8 and 19 nm, respectively (Fig. 2A).

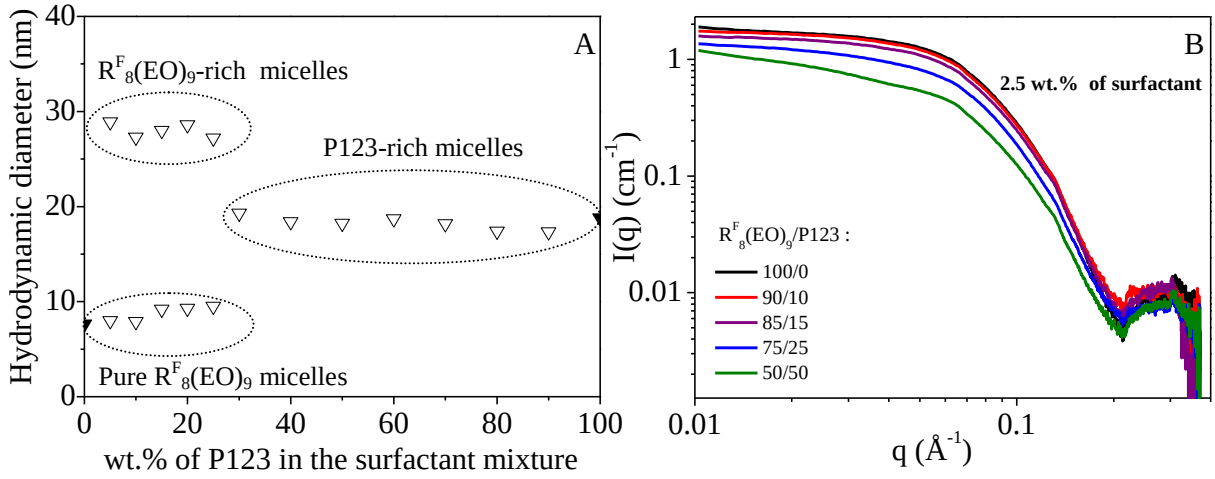

Figure 2 : Variation of the micelles hydrodynamic diameter (A) and evolution of the micelles SAXS profile (B) with the content of Pluronic in the surfactant mixture.

As observed on Figure 2, by incorporating P123 into the fluorinated solution, two sizes of micelles are observed by DLS up to a 25 wt.% of Pluronic. The first peak at around 8 nm can be attributed unambiguously to pure $R^F_8(EO)_9$ micelles. The second one at around 27 nm, larger than the radius of the pure P123 micelles (19 nm), is likely due to fluorinated micelles which have accommodated P123 molecules. Above a 25 wt.% of Pluronic only one size at around 18-19 nm is observed by DLS. This value is close to the size of the pure Pluronic micelles and it can be attributed to P123-rich micelles. It should be noted that, although above 25 wt.% of P123 the pure fluorinated micelles are not detected anymore by DLS, they are apparently present in the solution, as suggested by SAXS (Fig. 2B). Indeed, whatever the $R^F_8(EO)_9$/P123 weight ratio (90/10, 85/15, 75/25 and 50/50), the scattering curves roughly present the same feature and are comparable to the curve corresponding to the pure $R^F_8(EO)_9$ fluorinated micelles. As a first approximation, spectra have been described using a core/shell model with a fluorinated core radius of 1.0 nm and a total radius of 2.5 nm, as reported in a

previous study[40] dealing with the understanding by *in situ* SAXS of the formation mechanism of mesoporous materials templated by nonionic fluorinated micelles. Since the electronic density of fluorine is high, the contrast corresponding to the fluorinated micelles is so important that the signal due to the P123 micelles does not contribute to the scattering, reported in Figure 2B. Normalizing the spectra relatively to the volume fraction of the fluorinated surfactant, we can also note a slight gap towards lower intensities. This result indicates that the $R^F_8(EO)_9$ molecules not only participate on the formation of the pure fluorinated micelles, but a fraction of them is integrated in the micelles containing P123.

Meso-mesoporous materials from the CTM mechanism

First materials have been prepared under fluorinated conditions by keeping the $R^F_8(EO)_9$/P123 weight ratio to 90/10 and by changing the total concentration of surfactant, labeled as S bellow [S = $R^F_8(EO)_9$+P123], from 5 to 20 wt.%.

For S = 5 wt.%, two peaks at 10.9 and 5.3 nm are detected on the SAXS pattern (Fig. 3A). The last one is characteristic of the d_{100} reflection of a mesopore network templated by the fluorinated micelles[37]. Hence, the SAXS analysis shows the presence of two mesopore networks with two different pore sizes. Increasing the total surfactant concentration to 10 wt.%, two supplementary reflections at 6.4 and 5.6 nm appear on the SAXS pattern (Fig. 3A). The relative position between the peaks at 11.2, 6.4 and 5.6 nm is characteristic of a large mesopores hexagonal network having a cell parameter a_0 = 12.9 nm ($a_0 = 2d_{100}/\sqrt{3}$). The latter coexists with a smaller mesopores channel array templated by the fluorinated micelles, for which d_{100} is detected at 5.2 nm (a_0 = 6.0 nm). The existence of the two channel arrays is further evidenced by TEM analyses. Domains corresponding to small and large mesopores are observed on the TEM images depicted in Figure 3B.

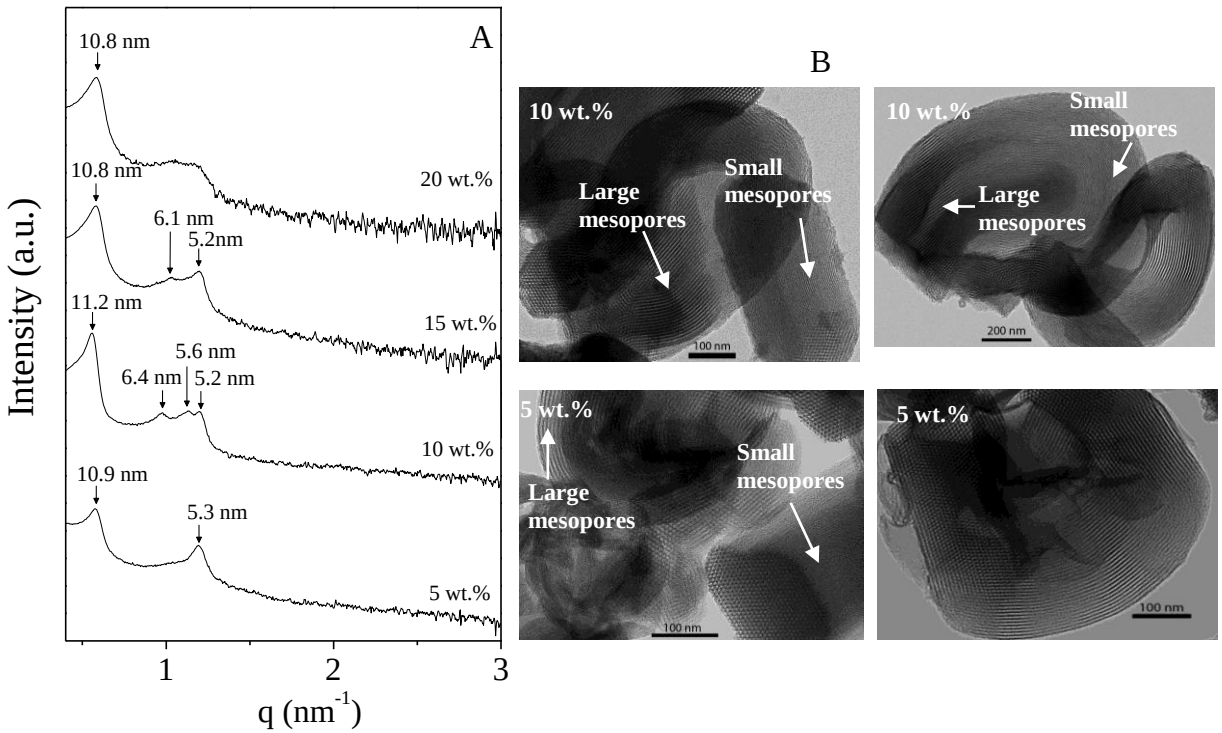

Figure 3 : SAXS pattern as function of the micellar concentration (wt.%) (A) and representative TEM images (B).

If S is further increased from 10 to 20 wt.%, the reflections characteristic of the large mesopores arrangement are less resolved, meaning that its disorganization has begun. In addition the d_{100} reflection (5.2 nm) arising from the smaller channel array becomes practically indistinguishable (Fig. 3A). Whatever S, the nitrogen adsorption-desorption isotherm exhibits two inflection points both during the adsorption and the desorption steps (Fig. 4A). This indicates the presence of two pore systems with different diameters. The dual-porosity is confirmed by the mesopore size distributions. Indeed, two peaks at around 3.4 and 9.6 nm, for S = 5wt.%, are clearly observed (Fig. 4B).

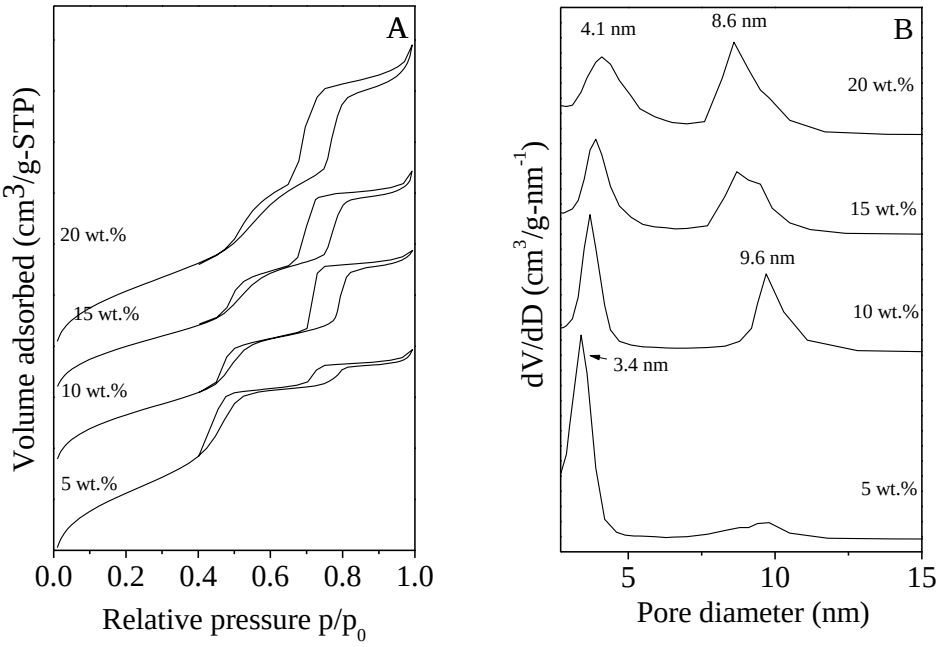

Figure 4 : Evolution of the nitrogen adsorption-desorption isotherms (A) and of the pore size distribution (B) as function of the micellar concentration (wt.%).

In that case, the micellar phase (L_1) is composed of two types of micelles: the pure $R^F_8(EO)_9$ micelles and $R^F_8(EO)_9$-rich micelles which have likely accommodated P123. Hence, when the silica source is added to the surfactant solution, it interacts with the two types of micelles leading to the formation of two organic-inorganic mesophases. During the material preparation, the silica source polymerizes both around the two kinds of micelles. Finally, the treatment at 80 °C completes the assembly and the polymerization of the silica source. After surfactant removal, dual-mesoporous materials are obtained.

With the increase of S, the capillary condensation of nitrogen within the smaller mesopores is less pronounced and from Figure 4B it appears that the population of the smaller pores decreases for the benefit of the bigger ones. This indicates that the fluorinated micelles are consumed to enrich the bigger micelles in fluorinated surfactant. Consequently, the association of $R^F_8(EO)_9$ and Pluronic in mixed micelles is favored when the global surfactant

concentration is raised and the system evolves to a situation where the Pluronic-rich micelles predominate. As a consequence, under the fluorinated conditions, the formation of the dual-mesoporous silica is not favored any longer above S = 20 wt.%. It should be noted that under these synthesis conditions, no material is recovered when the synthesis is carried out from a pure micellar solution of P123.

From SAXS it seems that the best mesopore ordering is obtained for S = 10 wt.%.

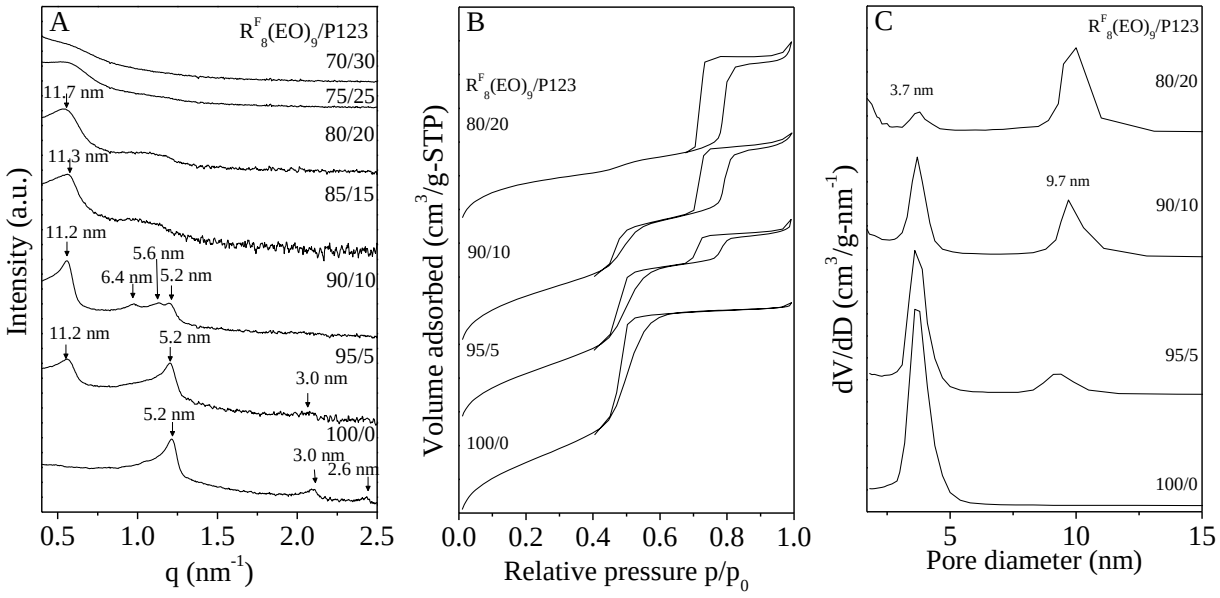

Figure 5 : Evolution of the SAXS pattern (A), the nitrogen-adsorption isotherms (B) and the pore size distributions (C) as a function of the $R^F_8(EO)_9$/P123 weight ratio. Materials have been synthesized under the fluorinated conditions with S = 10 wt.%.

However, for this concentration, increasing the P123 content in the surfactant mixture, as shown by Figure 5 the disorganization of the mesopore networks occurs and the dual mesoporosity disappears. In addition, for $R^F_8(EO)_9$/P123 weight ratios higher than 70/30, once again no material is recovered under these conditions. Therefore, we have investigated the formation of the meso-mesoporous materials under the Pluronic conditions. S has been fixed to 2.7 wt.%, concentration usually employed for the synthesis of SBA-15[37] and the

$R^F_8(EO)_{10}$/P123 weight ratio has been varied from 100/0 to 0/100. Using this synthesis procedure, for $R^F_8(EO)_9$/P123 weight ratios comprised between 0/100 and 25/75 the materials, exhibit a hexagonal mesopore ordering. Indeed the (100), (110) and (200) reflections at q ratios 1:√3:2 are clearly observed on the SAXS patterns (Fig. 6A).

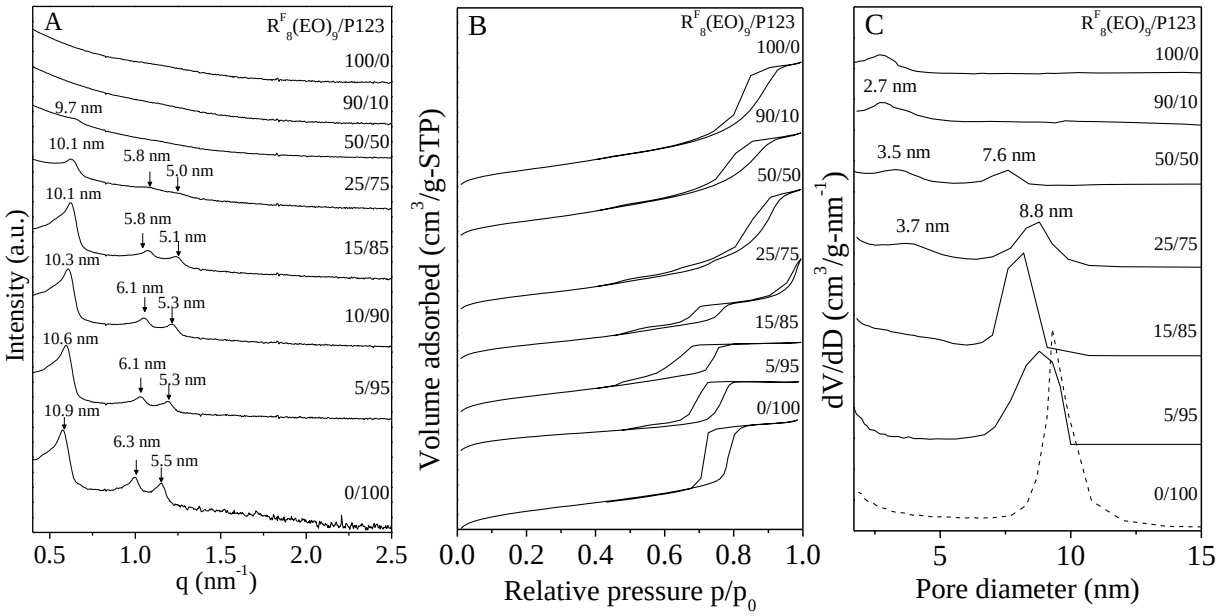

Figure 6 : Evolution of the SAXS pattern (A), the nitrogen-adsorption isotherms (B) and the pore size distributions (C) as a function of the $R^F_8(EO)_9$/P123 weight ratio. Materials have been synthesized under the Pluronic conditions with S = 2.7 wt.%.

Type IV isotherms with a H1 hysteresis loop by IUPAC classification[41] are obtained for these samples (Fig. 6B) and a narrow mesopore size distribution, centered at around 8-9 nm, is observed (Fig. 6C). This value is in accordance with the pore diameter of SBA-15[37] and it can thus be attributed to mesopores templating by P123 or P123-rich micelles.

If the weight fraction of P123 is decreased up to 0.50, the secondary reflection disappears (Fig. 6A). Beyond a 50/50 $R^F_8(EO)_9$/P123 weight ratio, no peak is detected anymore on the SAXS pattern and materials present a completely randomly pore arrangement. Therefore the CTM mechanism is not favored under these conditions in the presence of the fluorinated

micelles or fluorinated-rich micelles. However, it is interesting to note that for $R^F_8(EO)_9$/P123 weight ratios between 25/75 and 50/50 two distinct capillary condensation steps are clearly seen on the adsorption isotherm (Fig. 6B). The desorption branch also displays two distinct steps. This suggests the presence of two pore systems with distinct diameters, as shown by the pore size distribution which has two maxima at 3.7 and 8.8 nm (Fig. 6C). In the fluorinated surfactant-rich domain; i.e. for solutions containing a weight fraction of P123 lower than 0.50, only one inflection point is detected during the adsorption and the desorption steps (Fig. 6B) and the hysteresis is rather H2, which is often encountered for disordered materials. The component at around 8.8 nm disappears and the mesopore size distribution (Fig 6C) becomes similar to the one observed for the silica prepared by using the pure $R^F_8(EO)_9$, meaning that only the signature of the fluorinated micelles is observed, while being under the P123 conditions.

Meso-macroporous silica from emulsions

Hydrophilic fluorinated surfactant $R^F_8(EO)_9$ can lead to the formation of direct concentrated fluorinated emulsions with high stability, which can contain up to 98 wt.% of dispersed phase. In this study, to prepare highly concentrated oil-in-water (o/w) emulsions perfluorodecalin (PFD) has been incorporated into the mixed system containing $R^F_8(EO)_9$ and P123 and this micellar solution is constituted of both the pure fluorinated and the fluorinated-rich micelles . By this way, the PFD droplets, stabilized by the surfactant, are dispersed in the aqueous continuous media which is the micellar solution containing the two types of micelles. Porous materials have been templated by these emulsions. To do that, first a 10 wt.% micellar solution having a $R^F_8(EO)_9$/P123 weight ratio of 90/10 is prepared and then PFD is added. The concentration of oil incorporated to the micellar solution varied from 80 to 95 wt.%. For materials prepared with 80 and 85 wt.% of fluorocarbon, the two observed reflections reveal

the presence of two mesopores networks (fig. 7a). Indeed, the reflections at 11.8 and 6.9 nm indicate the formation of two disordered mesostructures, since the secondary reflections characteristic of the hexagonal ordering of the mesopores networks are not observed on the SAXS pattern (Fig. 7A). When increasing the PFD concentration to 90 and 95 wt.% only one reflection at 7.1 nm is detected by SAXS and the peak characteristic of the larger network disappears.

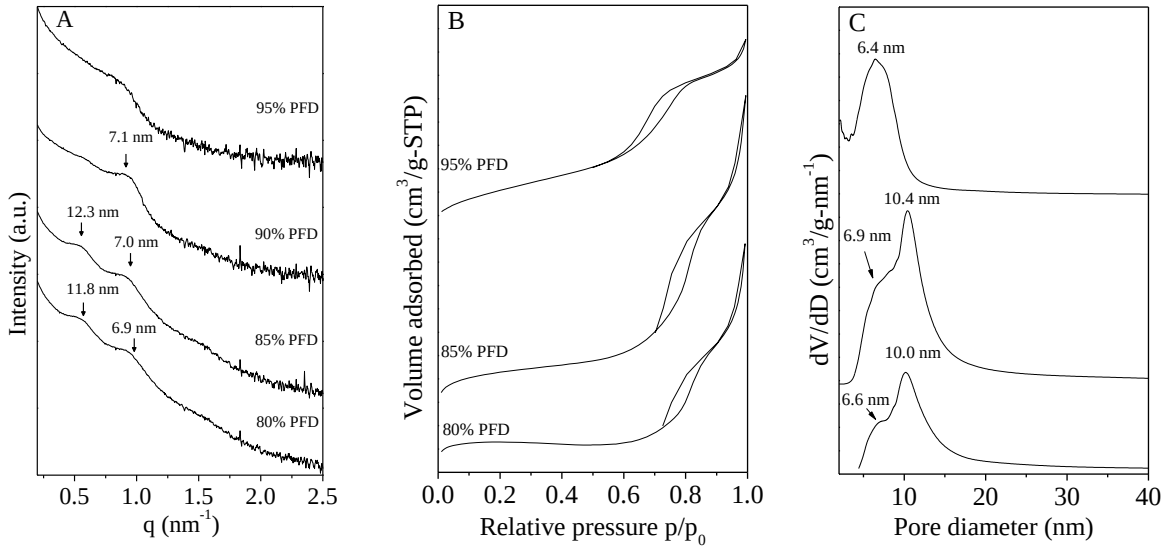

Figure 7 : SAXS pattern (A) and nitrogen adsorption-desorption isotherm (B) with the corresponding pore size distribution (C) of porous materials synthesized in the presence of PFD.

Upon the presence of PFD, a change of the shape of isotherms is observed (Fig. 7B). At high relative pressures (beyond $p/p_0 = 0.9$) the adsorbed volume of nitrogen does not remain constant as expected for type IV isotherms. This suggests the presence of macroporosity, either interparticular porosity or intrinsic macroporosity, due to the emulsion imprinting. Up to 85 wt.% of fluorocarbon, the mesopore size distribution clearly shows two maxima at around 6.6 and 10.0 nm (Fig. 7C). When increasing the PFD concentration to 90 and 95 wt.% materials exhibit a broad mono-modal mesopore size distribution centered at 6.4 nm (Fig.

7C). Comparing these materials with the ones synthesized without PFD, slightly higher values of mesopore diameter are obtained when PFD is present. This can be attributed to the swelling effect of PFD.

The formation of macropores templated by the emulsion is supported by both SEM (Fig. 8A) and TEM (Fig. 8B) analyzes.

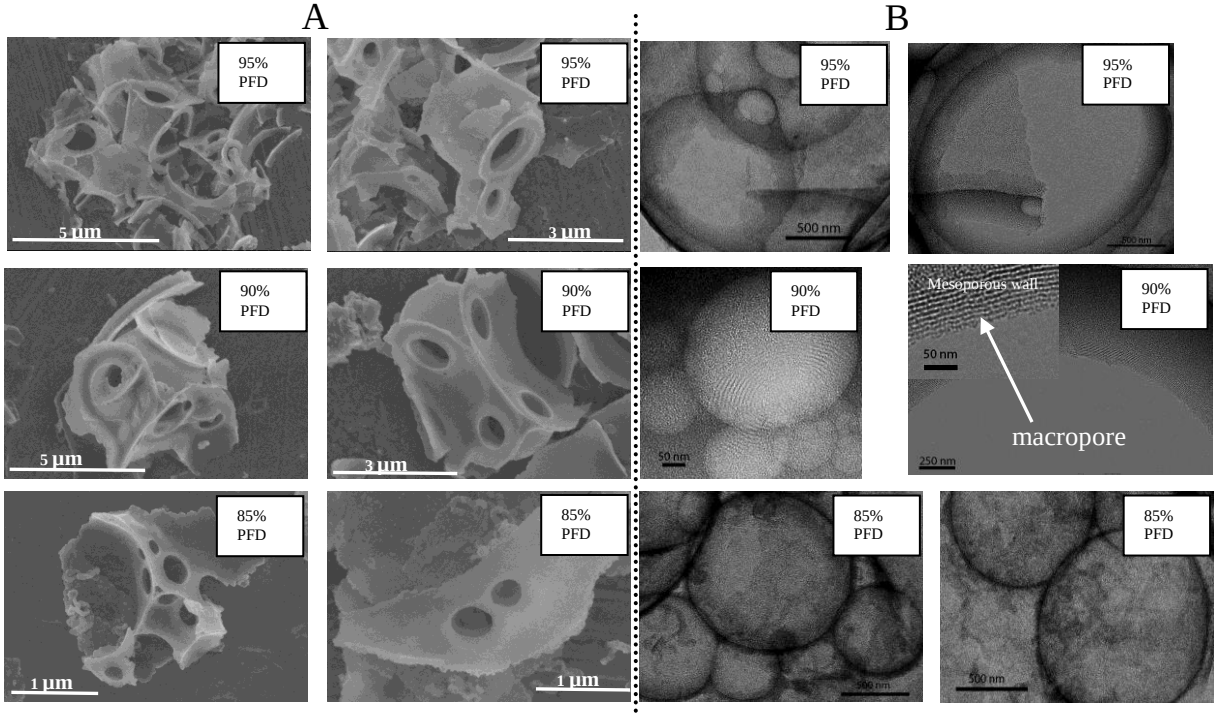

Figure 8: SEM (A) and TEM (B) images of materials synthesized in the presence of PFD.

Indeed, from Figure 8A, we can see that hollow spheres with apertures whose diameters are in the range of few microns are formed. These hollow spheres are broken, since after surfactant and oil removal the collapse of the structure occurred. TEM analysis also allows us to observe the macroporosity of the samples (Fig. 8B). Indeed, the imprints of the starting emulsion appear clearly on the images. Typically the macropore size is in the range of few microns, which is compatible with the size of the oil droplets. Moreover the mesoporosity is clearly evidenced in the wall of the macropores.

The presence of macropores in the samples was further confirmed by mercury intrusion experiments. Figure 9 shows the macropore size distribution of the samples prepared with 90 wt.% of oil.

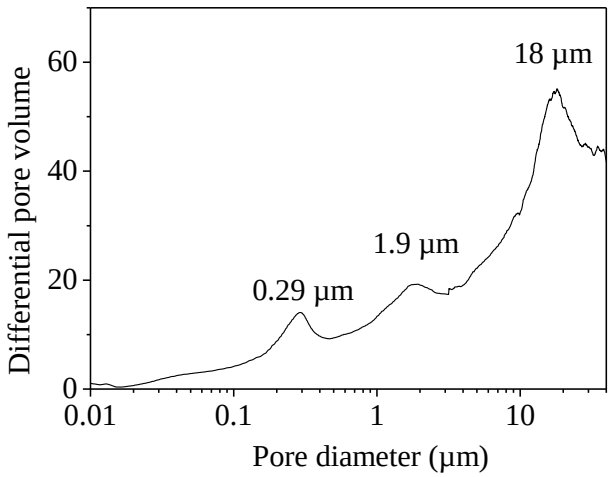

Figure 9 : Macropores size distributions.

The mercury intrusion porosimetry measurement reveals the presence of macropores with different size distributions centered at 0.29, 1.9 and 18 µm. The two first ones are in accordance with the size of the imprints of macropores observed on the SEM and TEM images (Fig. 8). The third peak situated at around 18 µm can arise from the interparticle porosity induced by the aggregation of particles.

Conclusion

Both $R^F_8(EO)_9$ and P123 surfactant solutions in water allow obtaining, in different synthesis conditions, ordered mesoporous materials, whose pore size is 4 and 10 nm, respectively. Previously in a short communication we have reported that the mixture of these two surfactants can be used to prepare materials meso-mesoporous silica by using a micellar solution with a global surfactant concentration of 10 wt.% and a $R^F_8(EO)_9$/P123 weight ratio of 90/10. Materials have been prepared under the conditions that give well ordered mesostructures using the pure fluorinated surfactant. Here, we have investigated in detail the effect of the mixed micelles composition, of the total surfactant concentration and of the synthesis conditions on the formation of the dual-mesoporous materials. So we have to consider not only the fluorinated conditions but also the Pluronic ones. Results show that keeping constant the proportion between the two surfactants and increasing the global

surfactant concentration, fluorinated micelles are consumed to enrich the bigger micelles in fluorinated surfactant and the mesopore ordering is progressively lost. The distribution between the two mesopore sizes is also reversed. In addition the dual-mesoporosity and the mesopore ordering are not favored when the materials are prepared under the Pluronic conditions. However, when the dual-mesoporosity is present, the DLS and SAXS analyzes reveal that whatever the synthesis conditions, the latter arises from the coexistence of the pure fluorinated micelles with either fluorinated-rich or Pluronic rich ones, depending on the Pluronic content in the surfactant mixture.

Upon the addition of PFD in the mixed surfactant system, concentrated emulsions can be formed and macro-mesoporous materials can be prepared by combining the CTM pathway with the emulsion templating mechanism.

Experimental section

The used fluorinated surfactant, which was provided by DuPont, has an average chemical structure of $C_8F_{17}C_2H_4(OC_2H_4)_9OH$. It is labeled as $R^F_8(EO)_9$. The hydrophilic chain moiety exhibits a Gaussian chain length distribution and the hydrophobic part is composed of well defined mixture of fluorinated tails. The selected triblock copolymer is the Pluronic P123 $(EO)_{20}(PO)_{70}(EO)_{20}$, which was purchased from Aldrich.

Phase diagram : The samples were prepared by weighting the required amounts of fluorinated surfactant, Pluronic and water in well-closed glass vials to avoid evaporation. They were left at controlled temperature for some hours in order to reach equilibrium. Liquid crystal phase domain was identified by its texture observed with optical microscope equipped with cross polarizers.

Dual-mesoporous material preparation: Meso-mesoporous materials have been prepared from the cooperative templating mechanism (CTM), according to synthesis procedures that

lead to the formation of well ordered mesopores networks by using pure $R^F_8(EO)_9$[37] or pure P123[38] as template, denoted below as fluorinated conditions and Pluronic conditions respectively. Tetramethoxysilane (TMOS) is used as the silica source and is added dropwise into the micellar solution at 20 °C.

Under fluorinated conditions, $R^F_8(EO)_9$ and P123 are mixed to form a micellar solution containing from 5 to 20 wt.% of surfactant in water. After addition of TMOS the solution is let under gentle stirring (150 rpm) for 1 hour. The surfactant/TMOS molar ratio and the pH have been fixed to 0.5 and 0.3, respectively. The $R^F_8(EO)_9$/P123 weight ratio was varied from 0/100 to 100/0. The treatment is performed during 1 day at 80 °C.

Under Pluronic conditions, the total surfactant concentration in water, the surfactant/TMOS molar ratio and the pH have been fixed to 2.7 wt.%, 0.017 and 0.3, respectively. The $R^F_8(EO)_9$/P123 weight ratio was varied from 0/100 to 100/0. After addition of TMOS and before performing the treatment at 100 °C during 48 hours, samples are aged during 24 hours at 40 °C. For example to prepare the material with a $R^F_8(EO)_9$/P123 weight ratio of 10/90 : 0.04 g of $R^F_8(EO)_9$ and 0.36 g of P123 are mixed to get a 2.7 wt.% micellar solution in water. Then 3.79 g of TMOS are added.

In both cases the final products are recovered after ethanol extraction with a Soxhlet apparatus during 48 hours.

Macro-mesoporous material preparation: Before the incorporation of perflurodecalin (PFD), the fluorinated oil, 0.9 g of $R^F_8(EO)_9$ and 0.1 g of P123 are dissolved in water (pH = 7) to form a micellar solution containing 10 wt.% of surfactant. The concentration of PFD, added to the micellar solution, varied from 80 to 95 wt.%. The mixtures were homogenized by stirring before the addition of the silica source at 20°C. The surfactant / silica molar ratio was fixed to 0.5. The obtained gel was sealed in Teflon autoclaves and heated during 1 day at 80°C. The

final products were recovered after ethanol extraction with a soxhlet apparatus during 48 hours.

Characterization: SAXS measurements of the powder samples were carried out using SAXSess mc2 (Anton Paar) apparatus. It is attached to a ID 3003 laboratory X-Ray generator (General Electric), equipped with a sealed X-ray tube (PANalytical, $\lambda_{Cu\ (K\alpha)}$ = 0.1542 nm, P = 3.3 kW). A multilayer mirror and a block collimator provide a monochromatic primary beam. A translucent beam stop allows the measurement of an attenuated primary beam at q = 0. Samples are introduced into a powder cell and placed inside an evacuated chamber. Acquisition times are typically in the range of 1 to 5 minutes. Scattering of X-ray beam is recorded by a CCD detector (Princeton Instruments, 2084 x 2084 pixels array with 24 x 24 µm² pixel size) in the q range 0.04 to 5 nm^{-1}. The detector is placed at 309 mm from the sample holder. All data were corrected for the background scattering from the empty cells. The SAXS measurements of the micellar solutions were recorded at the SWING SOLEIL beamline (energy 12 keV). The sample-CCD camera distance was 1.50 m, and the q range was from 6×10^{-3} to 0.5 $Å^{-1}$. The total surfactant concentration, 2.5 wt.%, has been chosen to overcome the interparticular interactions and thus to only observe the form factor of the micelles. The spectra were evaluated on an absolute scale and are plotted in the log-log representation. Samples for transmission electron microscopy (TEM) analysis were prepared by crushing some material in ethanol. Afterwards a drop of this slurry was dispersed on a holey carbon coated copper grid. A Philips CM20 microscope, operated at an accelerating voltage of 200 kV, was used to record the images. Scanning electron microscopy (SEM) was carried out with a HITACHI S-2500 at 15 keV. N_2 adsorption and desorption isotherms were determined on a Micromeritics TRISTAR 3000 sorptometer at –196 °C. The pore diameter and the pore size distribution were determined by the BJH (Barret, Joyner, Halenda)[39] method applied to the adsorption branch of the isotherm. Although it is well known that this

method gives an underestimated pore size, we use it here for the sake of simplicity and the use of this mathematical algorithm does not affect significantly our results as it is a systematic comparison. Dynamic Light Scattering (DLS) experiments were performed with a Malvern 300HSA Zetasizer instrument.

ACKNOWLEDGEMENTS:

Authors would like to thank DuPont de Nemours Belgium for providing the fluorinated surfactant and the SOLEIL synchrotron (SWING) for beam-time allocation. Anna May would like to thank the Spanish MICINN for the financial support within the framework of the project number CTQ2008-06892-C03-03/PPQ.

References

[1] C.S. Cundy, P.A. Cox, *Chem. Rev.* **2003**, *103*, 663-702.

[2] J.L. Vivero-Escoto, Y.D. Chiang, K.C.W. Wu, Y. Yamauchi, *Sci. Technol. Adv. Mater.* **2013**, *13*, 013003.

[3] F. Schüth, *Angew. Chem. Int. Ed.* **2003**, *42*, 3604-3622.

[4] K.C.W. Wu, Y. Yamauchi, *J. Mater. Chem.* **2012**, *22*, 1251-1256.

[5] P. Perego, R. Millini, *Chem. Soc. Rev.* **2013**, *42*, 3956-3976.

[6] Y.Wan, D. Zhao, *Chem. Rev.* **2007**, *107*, 2821-2860.

[7] D. Zhao, Q. Huo, J. Feng, B.F. Chmelka, G.D. Stucky, *J. Am. Chem. Soc.* **1998**, *120* 6024-3036.

[8] A. Firouzi, D. Kumar, L.M. Bull, T. Besier, P. Sieger, Q. Huo, S.A. Walker, J.A. Zasadzinski, C. Glinka, G.D. Stucky, *Science* **1995**, *267*, 1138-1143.

[9] Y.S. Lee, D. Sujardi, J.F. Rathman, *Langmuir* **1996**, *12*, 6202-6210.

[10] J.L. Blin, M. Impéror-Clerc, *Chem. Soc. Rev.* **2013,** *42*, 4083-4097.

[11] G.S. Attard, J.C. Glyde, C.G. Göltner, *Nature* **1995**, 378 (1995) 366-368.

[12] S.A. El-Safty, T. Hanaoka, *Chem. Mater.* **2004**, *16*, 384-400.

[13] S.A. El-Safty, Y. Kiyozumi, T. Hanaoka, F. Mizukami, *J. Phys. Chem. C* **2008**, *112*, 5476-5489.

[14] P. Feng, X. Bu, G.D. Stucky, D.J. Pine, *J. Am. Chem. Soc.*, **2000**, *122*, 994-995.

[15] K. Zimny, J.L. Blin, M.J. Stébé, *J. Phys. Chem. C* **2009**, *113*, 11285-11293.

[16] M.F. Ottaviani, A. Moscatelli, D. Desplantier-Giscard, F. Di Renzo, P. Kooyman, A. Galarneau, *J. Phys. Chem. B* **2004**, *108*, 12123-12129.

[17] L. Cao, T. Man , M. Kruk ,*Chem. Mater.* **2009**, *21*, 1144-1153.

[18] A. Sayari, Y. Yang, M. Kruk, M. Jaroniec, *J. Phys. Chem. B* **1999**, *103*, 3651-3658.

[19] A. Lind, J. Andersson, S. Karlsson, P. Ågren, P. Bussian, H. Amenitsch, M. Lindén, *Langmuir* **2002**, *18*, 1380-1385.

[20] J.L. Blin, M.J. Stébé, *Microporous and Mesoporous Mater.* **2005**, *87*, 67-76.

[21] J.L. Blin, M.J. Stébé, *J. Phys. Chem. B* **2004**, *108*, 11399-11405.

[22] C. Oh, S.C. Chung, S.I. Shin, Y.C. Kim, S.S. Im, S.G. Oh, *J. Colloids Interface Sci.* **2002**, *254*, 79-86.

[23] C. Zhao, E. Danish, N.R. Cameron, R. Kataku, *J. Mater. Chem.* **2007**, *17*, 2446-2453.

[24] S. Zhang, J. Chen, Polymer 48 (2007) 3021-3025.

[25] A. Keshavaraja, V. Ramaswamy, H.S. Soni, A.V. Ramaswamy, P. Ratnasamy, *J. Catal.* **1995**, *157*, 501-511.

[26] M.A. Parlett, K. Wilson, A.F. Lee, *Chem. Soc. Rev.* **2013**, *42*, 3876-3893.

[27] M.O. Coppens, G.F. Froment, *Fractals* **1997**, *5*, 493-505.

[28] B.T. Holland, L. Abrams, A. Stein, *J. Am. Chem. Soc.* **1999**, *121*, 4308-4309.

[29] J.L. Blin, A. Léonard, Z.Y. Yuan, L. Gigot, A. Vantomme, A.K. Cheetham, B.L. Su, *Angew. Chem., Int. Ed.* **2003**, *42*, 2872-2875.

[30] C.F. Blanford, H. Yan, R.C. Schroden, M. Al-Daous, A. Stein, *Adv. Mater.* **2001**, *13*, 401-407.

[31] T. Sen, G.J.T. Tiddy, J.L. Casci, M.W. Anderson, *Chem. Commun.* **2003**, *17*, 2182-2183.

[32] K. Nakanishi, Y. Kobayashi, T. Amatani, K. Hirato, Kodaira, *Chem. Mater.* **2004**, *16*, 3652-3658.

[33] H. Mori, M. Uota, D. Fujikawa, T. Yoshimura, T. Kuwahara, G. Sakai, T. Kijima, *Microporous and Mesoporous Mater.* **2006**, *91*, 172-180.

[34] O. Sel, D. Kuang, M. Thommes, B. Smarsly, *Langmuir* **2006**, *22*, 2311-2322.

[35] A. Imhof, D.J. Pine, *Nature* **1997**, *389*, 948-951.

[36] A. May, M.J. Stébé, J. M. Gutiérrez, J.L. Blin, *Langmuir* **2011**, *27*, 14000-14004.

[37] F. Michaux, M.J. Stébé, J.L. Blin, *Microporous and Mesoporous Mater.* **2012**, *151*, 201-210.

[38] T. Benamor, L. Vidal, B. Lebeau, C. Marichal, *Microporous and Mesoporous Mater.* **2012**, *153*, 100-114.

[39] E.P. Barret, L.G. Joyner, P.P. Halenda, *J. Am. Chem. Soc.* **1951**, *73*, 373-380.

[40] J. Schmitt, M. Impéror-Clerc, F. Michaux, J.L. Blin, M.J. Stébé, J.S. Pedersen, F. Meneau, *Langmuir* **2013**, *29*, 2007-2023.

[41] K.S.W. Sing, D.H. Everett, R.A.W Haul, L. Moscou, R.A. Pierotti, J. Rouquerol, T. Siemieniewska, T., *IUPAC, Pure and Appl. Chem.* **1985**, *57*, 603-619.

Graphical abstract

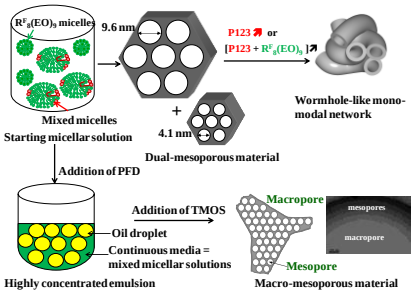

Table of content

Mixtures of polyoxyethylene fluoroalkyl ether and triblock copolymer are used to prepared hierarchical porous silica materials. Dual-mesoporous materials are obtained from the coexistence of two types of micelles through the cooperative templating mechanism and macro-mesoporous silica are templated by concentrated emulsions

Key topic

Hierarchical porosity/Mixed systems